Design and Implementation of a High Voltage Supply for Gridded Ion Thrusters using model-based control algorithms

IEPC-2019-409

Presented at the 36th International Electric Propulsion Conference
University of Vienna, Austria
September 15-20, 2019

Christian Roessler* and Uwe Probst†
THM, university of applied sciences, Giessen, Hessen, 35390, Germany

Peter J. Klar‡
University of Giessen, Giessen, Hessen, 35390, Germany

Abstract: Radio frequency ion thrusters (RIT) utilize a high voltage to extract ions out of the plasma. In order to generate this voltage on a satellite system its power bus voltage needs to be raised. This task can be performed by means of a FPGA controlled push-pull converter type that is presented within this paper. The theory of estimating output voltage and current in order to control that type of high voltage generator will be provided. It is intended to be used as an alternative approach compared to the challenging direct measurement of the converter's output values but could be utilized as a backup solution as well. The accuracy of the grid voltage is crucial for reducing grid erosion and extend the thruster's lifetime. The provided current value can be utilized to detect a short circuit inside the grid system or as a measure of the generated thrust either.

Nomenclature

S_x	= Operating State of the converter
PS	= Phase Shift
N	= Transformer turns ratio (secondary turn count divided by primary turn count)
L_m	= magnetizing inductance of the transformer
L_σ	= primary sided leakage inductance of the transformer
V_out	= converters output voltage
I_out	= converters output current
v_bridge	= full bridge inverter output voltage
i_bridge	= full bridge inverter output current
$\frac{di_\mathrm{bridge}}{\mathrm{dt}}$	= slope of the bridge current
v_p	= voltage across ideal transformers primary winding
v_sec	= transformer output voltage
i_p	= primary ideal transformer current
i_sec	= secondary ideal transformer current
v_DC	= input voltage of the converter
t_p	= switching period of the full bridge inverter

*Research Assistant, Department of Electrical Engineering, christian.roessler@ei.thm.de
†Professor, Department of Electrical Engineering, uwe.probst@ei.thm.de
‡Professor, Institute of Experimental Physics I, peter.j.klar@exp1.physik.uni-giessen.de

I. Introduction

The university of applied sciences in collaboration with the university of Giessen are investigating in technologies all around the Radio Frequency Ion thruster (RIT). Fundamental concepts based on new technologies for efficient and reliable Radio-frequency Generators (RFGs) and Power Processing Units (PPUs) are one part of their research area. Our test facility allows the operation of thrusters up to a RIT-10 in conjunction with developed electronic assemblies for testing and evaluation purposes. However, some of the developed concepts are not restricted to be used in RIT-Systems only. Especially the generation of a high voltage boosting the satellite bus voltage to meet the individual thruster requirements is necessary in HET- and HEMP-Systems, too. Increasing the efficiency of that energy conversion process is a primary objective during the design since it reduces the dissipated power and simplifies the integration into a superordinate thruster system regarding its thermal design. Furthermore the component stresses can be reduced due to lower temperatures. This impacts both lifetime and reliability in a positive manner.

Focussed on a gridded ion thruster an increased extraction voltage affects the specific impulse leading to a better mass efficiency. Further on a dual stage acceleration is conceivable[2] but needs an additional high voltage supply. To prevent erosion in the grid system due to an unfocused ion beam precise adjustment of the converter's output voltages is essential for these types of thrusters. In addition the measure of grid currents provided by the high voltage supplies can be used not only to ensure optimal beam focus but also to estimate the generated thrust. However, measuring the output voltage and current of a galvanically isolated power supply increases the coupling capacity across the separated voltage domains and reduces the quality of isolation. This effect becomes more significant the higher extraction voltages rise.

The basic idea of estimating the output voltage and current of a high voltage supply is to calculate these parameters from easy to measure quantities. The electrical effort required to record these values is small compared to the direct measurement and does not influence the galvanical isolation. Based on available system parameters the desired values can be calculated online and provided to a control instance. This approach can be used either instead of direct measurements or in parallel to increase the redundancy and improve the system reliability. In case of sensor failure the output values can still be calculated and closed loop control is ensured.

Especially the method of output voltage and current estimation is a major part within this paper. The basic operation of the circuit topology and its control method is described in the following section. Hereafter the theory of output parameter estimation is presented and evaluated using simulations.

II. Power Stage Design

To generate the desired high output voltage a push-pull-converter according to Fig. 1 is used. From the power electronics point of view the circuit can be divided into four major parts: Full-Bridge-Inverter, high-frequency transformer, rectifier with filter and the attached load represented by an ohmic resistance. Supplied by the satellite bus voltage in the range of 20V - 30V DC [3] an alternating voltage pattern is formed using four mosfets in full-bride configuration. The output voltage and current of the inverter are referred to as v_{bridge} and i_{bridge} respectively. Fig. 2 shows the corresponding waveforms including the mosfet control signals. The entire operation sequence can be divided into four states S_1 to S_4. During S_1 and S_3 the input voltage is applied to the transformer's primary and causes the bridge current to rise. Now energy is transferred from the input source v_{dc} to the output. When entering the states S_2 and S_4 the bridge voltage becomes zero and the current is free wheeling driven by the inductances of the transformer only. Adapting the phase shift (PS) between the control signals of the two individual half bridges will modify the ON-time of S_2 and S_4 and so affect the output voltage of the converter. In order to achieve a voltage increase, a high-frequency transformer is used. The turns ratio between secondary and primary winding count is referred to as N. The transformer model consists of the mutual inductance L_{m} as well as the primary leakage inductance L_σ. These elements are important for calculating the output voltage and current respectively. The consideration of the primary leakage inductance is also indispensable to realize a control algorithm in order to minimize switching losses depending on the operating point (ZVS)[4]. A full bridge rectifier consisting of high voltage silicon carbide (SiC) diodes provides DC output voltage. A subsequent filter capacitor C_{F} is used for smoothing the output voltage provided to the load resistor.

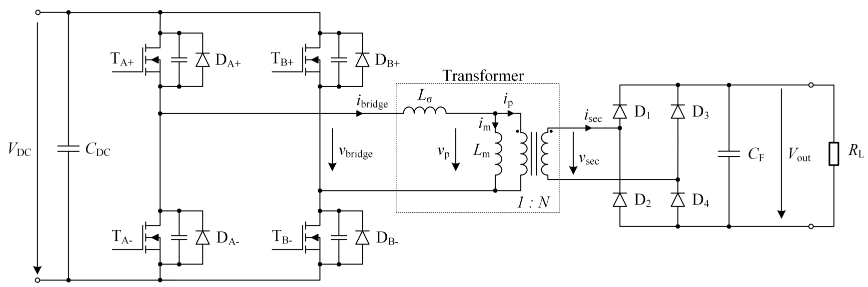

Figure 1. Equivalent circuit model of the utilized push-pull-converter

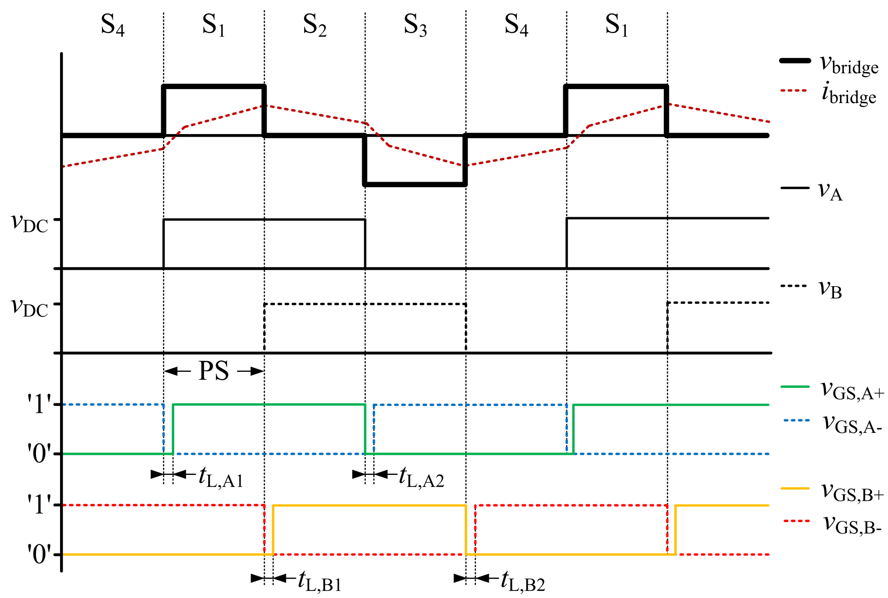

Figure 2. Full bridge waveforms and control signals

A. Output voltage estimation

To derive the output voltage the circuit model according to Fig. 1 is analyzed. To start with continuous current mode (CCM) depicted in Fig. 3 will be discussed. The substantial condition to operate in CCM are the primary transformer current or the transformed value i_{sec} respectively. CCM is ensured as long as i_{sec} does not drop down to zero during a free wheeling state S_2 or S_4 before a subsequent energy transfer state S_1 or S_3 is applied. In CCM the bridge current consists of three different current slopes during S_1 and S_2. These slopes strongly depend on the conductance state of the rectifier diodes D_1 to D_4. At the beginning of S_1 i_{bridge} is negative. Assuming the magnetizing current to be much smaller compared to i_{bridge}, the primary current is almost equal to i_{bridge} and Eqn. 1 is a valid simplification:

$$i_{\text{p}} = i_{\text{bridge}} - i_{\text{m}} \approx i_{\text{bridge}} \tag{1}$$

In this case i_{p} is negative as well. Taking into account the winding polarity i_{sec} can be determined according to Eqn. 2.

$$\begin{bmatrix} v_{\text{sec}} \\ i_{\text{sec}} \end{bmatrix} = \begin{bmatrix} N & 0 \\ 0 & \frac{1}{N} \end{bmatrix} \cdot \begin{bmatrix} -v_{\text{p}} \\ -i_{\text{p}} \end{bmatrix} \tag{2}$$

The sign of i_{sec} specifies which diodes conduct, D_1/D_4 and D_2/D_3 respectively. In case of D_1/D_4 the output voltage is applied to the secondary side of the transformer and transformed to the primary. So the primary voltage can be determined as

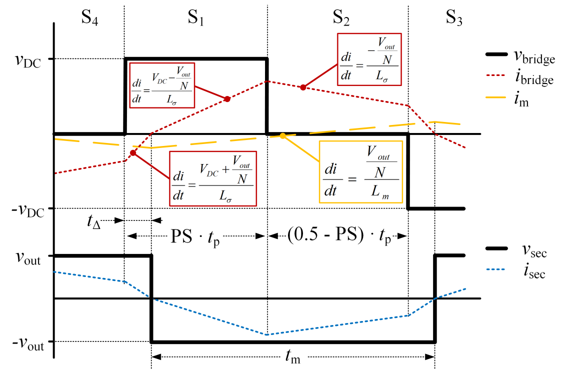

Figure 3. Bridge and secondary waveforms during CCM operation of the converter

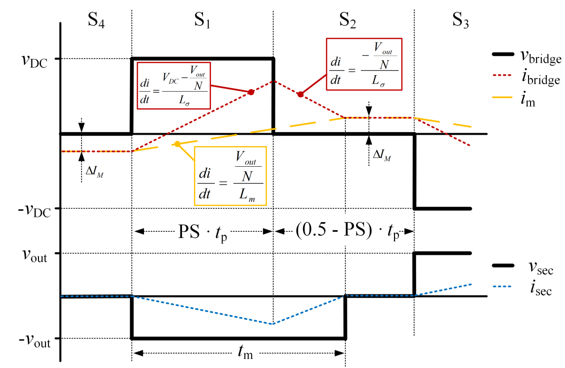

Figure 4. Bridge and secondary waveforms during DCM operation of the converter

$$v_{\mathrm{p}} = \frac{v_{\mathrm{sec}}}{N} = \frac{v_{\mathrm{out}}}{N}. \tag{3}$$

Since v_{bridge} is constant during S_1 the voltage drop across L_σ can be calculated. Hence, the first slope of i_{bridge} during S_1 turns out as follows:

$$\frac{di_{\mathrm{bridge}}}{dt} = \frac{v_\sigma}{L_\sigma} = \frac{v_{\mathrm{bridge}} - v_{\mathrm{p}}}{L_\sigma} = \frac{V_{\mathrm{DC}} - (-\frac{V_{\mathrm{out}}}{N})}{L_\sigma} = \frac{v_{DC} + \frac{v_{out}}{N}}{L_\sigma} \tag{4}$$

The negative sign in Eqn. 4 in $-\frac{V_{\mathrm{out}}}{N}$ is a consequence of the transformers winding polarity and due to that a consistent application of the ideal transformer type coupling in Eqn. 2. Changing the polarity of one transformer winding does not influence the described principles. The remaining slopes of i_{bridge} can be calculated in a similar manner using v_{bridge} and v_{out}. Results are given in Fig. 3. Therefore, measuring the slope of i_{bridge}, V_{out} can be calculated if the DC link voltage, the leakage inductance, the turns ratio and the present state S_1 to S_4 are known.

The slope of the magnetizing current can be determined from Fig. 3 also. It is useful to detect whether the circuit is operating in CCM or in the corresponding discontinuous current mode (DCM) shown in Fig. 4.

B. Discontinuous current mode

If i_{sec} and as a consequence v_{sec} become zero before the next state is applied, the mode of operation is referred to as discontinuous current mode (DCM) and shown in Fig. 4. Neglecting any ohmic losses i_{bridge} is equal to the magnetizing current until S_1 or S_3 is applied. Using the waveforms of i_{bridge} and i_{m} the values ΔI_{m} and t_{m} are given by Eqn. 5 and Eqn. 6.

$$\Delta I_{\mathrm{m}} = \frac{t_{\mathrm{p}} \cdot PS \cdot V_{\mathrm{DC}}}{(L_\sigma + L_{\mathrm{m}}) \cdot 2} \tag{5}$$

$$t_{\mathrm{m}} = \frac{t_{\mathrm{p}} \cdot PS \cdot V_{\mathrm{DC}} \cdot N \cdot L_{\mathrm{m}}}{V_{\mathrm{out}} \cdot (L_\sigma + L_{\mathrm{m}})} \tag{6}$$

t_m describes the interval when i_m changes and a voltage is applied across the ideal transformer's primary and secondary windings. In order to ensure CCM operation the interval t_m must be greater than or equal to $\frac{t_p}{2}$. The corresponding condition is given in Eqn. 7.

$$\frac{PS \cdot v_{DC} \cdot N \cdot L_m}{v_{out} \cdot (L_\sigma + L_m)} \geq 0.5 \tag{7}$$

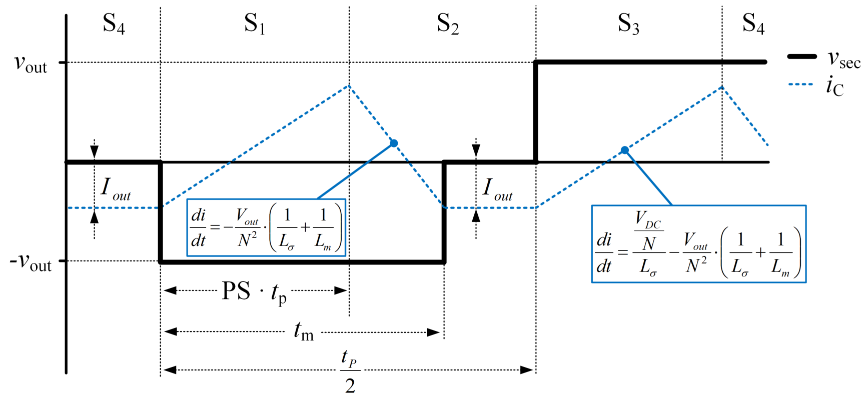

Figure 5. Waveforms of transformer secondary voltage and current of filter capacitor during DCM operation

C. Output current estimation

Assuming the output voltage is known using the method of current slope determination the output current can be calculated similarly. For DCM, the waveform of i_c is depicted in Fig. 5. Assuming both the output voltage as constant and an ohmic load resistor, the output current I_{out} is a pure dc current. It is comprised of the rectified secondary current as well as the output capacitor's current according to kirchhoff's first law. If i_{sec} drops to zero the entire output current is provided by the capacitor C_{F}. According to Fig. 5 this current can be found at the end of S_2 and S_4 reflected in a constant i_{C}. The first current slope of i_{C} during S_2 is equal to the slope of i_{sec} which in turn is equal to the transferred primary current slope of i_{p}. This relation can be expressed by the following Eqn. 8.

$$\frac{di_C}{dt} = \frac{di_{\text{sec}}}{dt} = \frac{di_p}{dt} \cdot \frac{1}{N} = (-\frac{\frac{v_{out}}{N}}{L_\sigma} - \frac{\frac{V_{\text{out}}}{N}}{L_m}) \cdot \frac{1}{N} = \frac{V_{\text{out}}}{N^2} \cdot (\frac{1}{L_\sigma} + \frac{1}{L_m}) \tag{8}$$

Eqn. 8 is only valid in S_2 and S_4. The slopes of i_{c} during S_1 and S_3 can be derived accordingly. Considering I_{out} as unknown parameter and using the calculated slopes of i_{C} a linear system of equations can be derived. Taking into account that i_{C} is a pure alternating signal the integral during $\frac{t_{\text{p}}}{2}$ has to vanish. As a result the system can be solved completely and an expression for I_{out} in DCM operation is found in Eqn. 9.

$$I_{\text{out,DCM}} = \frac{t_p \cdot PS^2 \cdot V_{\text{DC}}^2 \cdot L_H}{L_\sigma \cdot V_{\text{out}} \cdot (L_\sigma + L_m)} - \frac{t_p \cdot PS^2 \cdot V_{\text{DC}}}{L_\sigma \cdot N} \tag{9}$$

During CCM calculation of I_{out} can be done also. Fig. 6 shows the corresponding waveforms used to derive the analytical expression. Similar to DCM operation the capacitor current i_{C} is a pure alternating signal. Consequently the integral of i_C has to vanish within the boundary of $\frac{t_{\text{p}}}{2}$. The current slopes during the different states are developed as explained before and shown in Fig. 5. To solve the system of equations completely the parameter t_Δ is required. It defines the interval between entering of State S_1 or S_3 and the moment i_{bridge} crosses zero. It is referred to in Fig. 3 and given Fig. 6 as well. The expression of t_Δ can be derived using i_{bridge} during CCM operation and is shown in Eqn. 10.

$$t_\Delta = \frac{t_p}{2} \cdot PS - \frac{t_p}{4} \cdot \frac{V_{\text{out}}}{V_{DC} \cdot N} \tag{10}$$

In CCM v_{sec} and v_p respectively are never zero hence the magnetizing period t_m is equal to $\frac{t_p}{2}$. This relation can be used to create an alternative expression for V_{out}, shown in Eqn. 11

$$V_{out} = 2 \cdot \frac{PS \cdot N \cdot L_m \cdot V_{DC}}{(L_\sigma + Lm)} \tag{11}$$

The final result of $I_{\text{out,CCM}}$ is represented by Eqn. 12:

$$I_{\text{out,CCM}} = \frac{t_p}{2} \cdot (\frac{\frac{V_{\text{DC}}}{N}}{L_\sigma} - \frac{PS \cdot V_{DC}}{(L_\sigma + L_m) \cdot N} - \frac{PS^2 \cdot L_m^2 \cdot V_{DC}}{(L_\sigma + L_m)^2 \cdot L_\sigma \cdot N}) \tag{12}$$

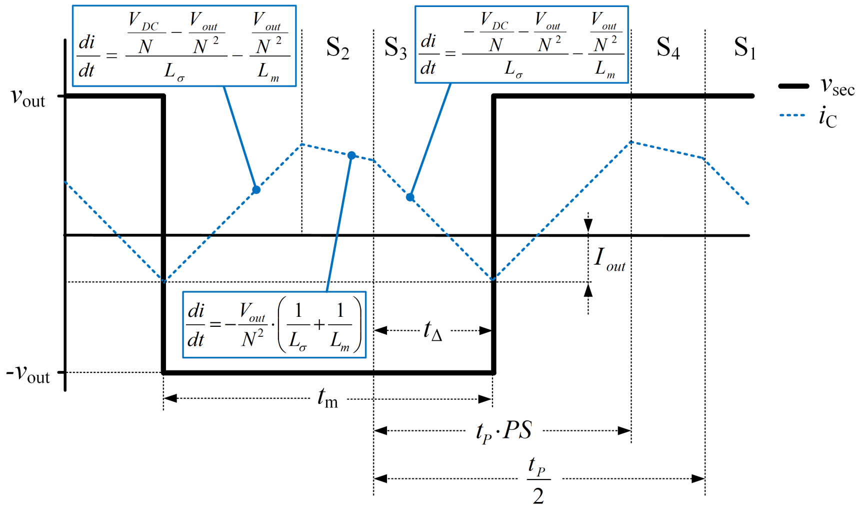

Figure 6. Waveforms of transformer secondary voltage and current of filter capacitor during CCM operation

III. Conclusion and outlook

Within this paper a method of output voltage and output current estimation is shown. The theory has been inferred using a full bridge push-pull converter topology operated as a high voltage generator. Simulations were used to verify the developed relations. According to the electrical model in Fig. 1 certain assumptions have been made to simplify the problem. In this regard the transformer's secondary leakage inductance is neglected as well as the entire ohmic losses of power semiconductors and transformer. In order to improve calculation accuracy these effects must be taken into account. Furthermore the output voltage is considered as constant but actually includes a ripple voltage.

Implemented inside a FPGA the presented relations are intended to be used as a basis for an observer controlled power supply. A further objective is to handle the nonlinearity of magnetizing inductance to ensure the accurate estimation of output voltage and current. The acquisition of L_m on startup of the converter or during operation is a further task in the development of the proposed system.

References

[1] Sabate, J. A., Vlatkovic, V., Ridley, R. B., Lee, F.C. and Cho, B. H., "Design Considerations For High-Voltage High-Power Full-Bridge Zero-Voltage-Switched PWM Converter," Virginia Power Electronics Center, 1990

[2] Bramanti, C., Walker, R., Sutherland, O., Boswell, R., Charles, C., Fearn, D., Amo, J. G. D., Orlandi, M., "The Innovative Dual-Stage 4-Grid Ion Thruster Concept - Theory And Experimental Results", International Astronautical Congress, IAC-06-C4.4.7, 2006

[3] Leiter, H. J., Altmann, Ch., Kukies, R., Kuhmann, J., Porst, J.-P., Berger, M., Rath, M., "Evolution of the AIRBUS DS GmbH Radio Frequency Ion Thruster Family", Joint Conference of 30th International Syposium on Space Technology and Science, 34th International Electric Propulsion Conference and 6th Nano-satellite Symposium, IEPC-2015-90/ISTS-2015-b-90, Hyogo-Kobe, Japan, 2015

[4] Roessler, C., Probst, U., Simon, J., Klar, P. J., "Development of a controlled High Voltage Power Supply for Gridded Ion Thrusters", 35th International Electric Propulsion Conference, IEPC-2017-337, Atlanta, Georgia - USA, 2017